Houlsby, G. T., Kelly, R. B., Huxtable, J. & Byrne, B. W. (2006). *Géotechnique* **56**, No. 1, 3–10

Field trials of suction caissons in sand for offshore wind turbine foundations

G. T. HOULSBY*, R. B. KELLY†, J. HUXTABLE‡ and B. W. BYRNE*

A programme of testing on suction caisson foundations in an artificially prepared sand test bed near Luce Bay, in Scotland, is described. The tests are relevant to the design of either monopod or quadruped foundations for offshore wind turbines. Records are presented for suction installation of the caissons, cyclic moment loading under both quasi-static and dynamic conditions to simulate the behaviour of a monopod foundation, and cyclic vertical loading and pullout of caissons to simulate one footing in a quadruped foundation. Variations of stiffness with loading level of the foundation are observed, with high initial stiffness followed by hysteretic behaviour at moderate loads and degradation of response at high loads. Some implications for the design of wind turbine foundations are briefly discussed.

KEYWORDS: bearing capacity; dynamics; footings/foundations; sands; stiffness

Nous décrivons un programme d'essais réalisé sur des fondations à caisson de succion dans un banc de sable préparé artificiellement près de Luce Bay, en Écosse. Ces essais sont importants pour la conception de fondations à un seul ou à quatre pieds de turbines d'éoliennes offshore. Nous présentons les chiffres pour l'installation de succion des caissons, la charge de moment cyclique en conditions quasi-statiques et dynamiques pour simuler le comportement d'une fondation à un seul pied, et le chargement et arrachement cycliques verticaux des caissons pour simuler un pied dans une fondation quadrupède. Nous observons les variations de rigidité en fonction du niveau de chargement de la fondation, une rigidité initiale élevée étant suivie par un comportement d'hystérésis sous charges modérées et une dégradation de la réponse sous charges élevées. Nous examinons brièvement certaines implications pour la conception de fondations de turbines éoliennes.

INTRODUCTION

The offshore wind energy industry is a very rapidly expanding sector of vital economic importance in the UK, and the foundation represents an important part of the costs of offshore wind turbine installations (Byrne & Houlsby, 2003). This paper describes a series of tests directed towards the understanding of the behaviour of suction caisson foundations in sand, as possible foundations for offshore wind turbines.

An earlier paper, by Houlsby *et al.* (2005c), describes in detail the background motivation to this testing, and presents equivalent data for tests in clay. The key purpose of this testing is to provide data at a scale that can be used to extrapolate from laboratory-scale tests to prototype design. These data complement a significant test programme carried out in the laboratory at Oxford University and described in papers by Byrne & Houlsby (2002, 2003, 2004) and Houlsby *et al.* (2005a). The derivation and application of scaling relationships to the field and laboratory data are described in detail by Houlsby *et al.* (2005d). The testing programme described here follows a similar pattern to the tests in clay (Houlsby *et al.*, 2005c), and includes tests directed towards the design of both monopod and quadruped foundations for offshore wind turbines. The most important load case for a monopod foundation is the applied overturning moment, whereas for a quadruped foundation the vertical loading on an individual caisson is most important. Data were obtained from the installation phases for each caisson. Loading of the caissons was by means of a combination of dead weights, hydraulic jacks and inertial loading from a structural eccentric mass vibrator (SEMV). The test programme was designed by Oxford University, and site operations were managed by Fugro Structural Monitoring Ltd. The tests were carried out in February and March 2004.

Manuscript received 27 October 2004; revised manuscript accepted 17 October 2005.
Discussion on this paper closes on 3 July 2006, for further details see p. ii.
* Department of Engineering Science, Oxford University, UK.
† Coffey Geosciences, Australia, Formerly Oxford University, UK.
‡ Fugro Structural Monitoring Ltd, Glasgow, UK.

THE LUCE BAY TEST SITE

The tests were carried out in a specially prepared sand bed in an aggregate extraction quarry near Luce Bay, Dumfries and Galloway, Scotland. The bed was prepared by placing selected fill in layers approximately 250 mm thick and compacting them by multiple passes of a wheeled loader. The sand bed was approximately 40 m × 15 m × 3·5 m deep. A grading curve for the sand is shown in Fig. 1. Although the sand itself is almost single-sized at about 0·3–0·4 mm, it can be seen that there is a significant (15%) gravel content. The sand bed was also observed to contain a proportion of small, rounded stones up to about 80 mm in size, even though every attempt was made to remove this coarser material in the preparation of the bed. The fines content is negligible. The fill was placed in an unsaturated condition above the water table in the summer. The entire sand bed was allowed to flood slowly over a period of several months, and by the time of the testing had been submerged for four months. During testing there was about 150 mm depth of water over the sand surface.

The bed of sand was characterised principally by means of in situ testing. Three cone penetration tests (CPT) with pore pressure measurement, two cone pressuremeter tests and three seismic cone tests were conducted. The cone resistance records of three CPT and two cone pressuremeter tests are shown superimposed in Fig. 2, showing (within some variability) a strong increase of cone resistance with depth, due principally to the increasing stress level. Using standard correlations, the estimated relative density of the sand bed was 80–85%. In the lower part of the sand layer there appears to be some looser material, and beneath the sand are much softer deposits that were not investigated in detail.

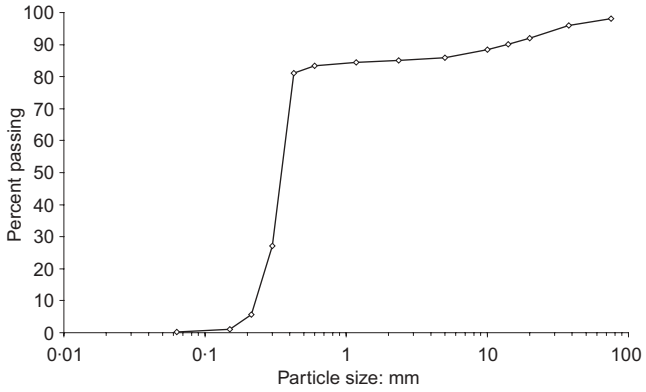

Fig. 1. Grading curve for test bed at Luce Bay

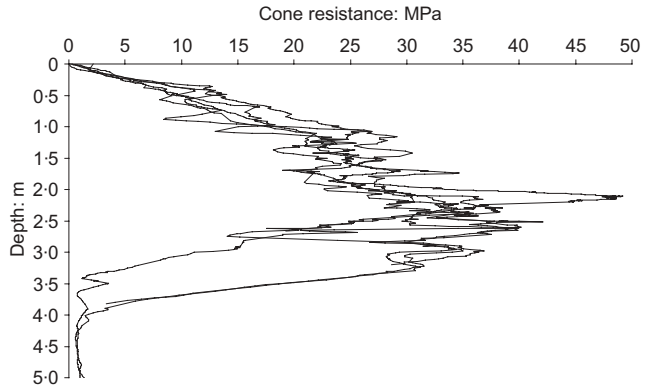

Fig. 2. CPT data at Luce Bay

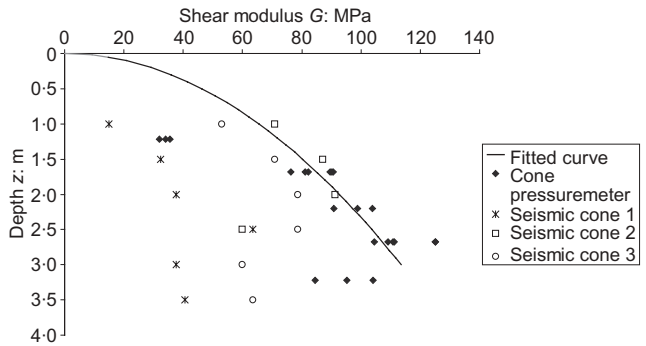

Fig. 3. Estimated profile of shear modulus with depth at Luce Bay

Figure 3 shows profiles of shear modulus with depth inferred from the cone pressuremeter and seismic cone tests. The data from the seismic cone are representative of the very-small-strain shear modulus. The data from the cone pressuremeter were from unload–reload loops with an amplitude of hoop strain at the pressuremeter surface of approximately 0·25%, but will be representative of the behaviour at smaller strains, because the strain amplitude in the soil reduces inversely with the radial distance from the pressuremeter. Down to a depth of 2 m there is generally good agreement between the seismic and cone pressuremeter data, with the exception of that from seismic cone test 1. At greater depths, the cone pressuremeter data suggest a higher shear modulus than the seismic cone data. The shear stiffness can be characterised by the relationship $G/p_a = 2500\sqrt{p'/p_a}$, where p_a is atmospheric pressure and p' is the mean effective stress estimated using a saturated unit weight of 10·3 kN/m^3 and the coefficient of earth pressure at rest, K_0, as 0·5. Although the choice of K_0 value is arbitrary, the calculation itself is relatively insensitive to the precise value. This relationship has been fitted to the upper bound of the test data, as disturbance during testing was expected to lead to underestimates of the small-strain shear modulus. We note, however, that the shear moduli observed at this site are quite high for sand at shallow depths, and this may be due to the compaction procedures used in preparation of the bed.

EQUIPMENT AND TESTING PROCEDURES

The caissons, loading frame and instrumentation methods used for the tests in sand were essentially identical to those employed in the previous clay tests at Bothkennar (Houlsby *et al.*, 2005c). A caisson of diameter 3·0 m and with a skirt 1·5 m deep was used for moment loading tests. A second caisson of diameter 1·5 m and with a 1·0 m skirt was used for vertical loading tests. An outline diagram of the test set-up is given in Fig. 4, and a photograph of the rig installed at the Luce Bay testing site is shown in Fig. 5.

Prior to suction-assisted installation the caissons were allowed to penetrate under their own weight, with the vent to the caisson open to air. In the case of the 3 m caisson a 2400 kg mass was added to the caisson to cause a slight further penetration. The caisson vent was then closed and suction applied by pumping out the trapped air from inside the caisson. The pump used was capable of pumping both air and water. A flow meter was installed between the caisson and pump.

The testing procedures in sand were very similar to those adopted for the tests in clay (Houlsby *et al.*, 2005c). The principal exception related to the SEMV tests using a structural eccentric mass vibrator to apply relatively high-frequency cyclic loading. Experience from the earlier clay tests indicated the value of having a spread of data obtained at different frequencies of loading. At Luce Bay a series of tests were therefore carried out, in which the frequency was increased in steps, with approximately 15 s of cycling at each frequency. A more reliable definition of the variation of the complex impedance with frequency was possible using this method.

The 1·5 m and 3·0 m caissons were each installed and tested at two locations in the test bed at Luce Bay: a brief summary of the tests completed is given in Table 1.

TEST RESULTS

Installation

Figure 6 shows the records of measured suction against penetration depth for one installation of the 3·0 m caisson and one of the 1·5 m caisson. It can be seen that the variation of the required suction with depth is similar for both caissons. Also shown in the figure are the computed profiles of suction, using the procedure described by Houlsby & Byrne (2005)

$$V' + s\left(\pi D_i^2/4\right) = \int_0^h \sigma'_{vo}\mathrm{d}z\ (K\tan\delta)_o(\pi D_o) + \int_0^h \sigma'_{vi}\mathrm{d}z\ (K\tan\delta)_i(\pi D_i) + \left(\sigma'_{vi}N_q + \gamma' tN_\gamma\right)(\pi Dt) \quad (1)$$

The subscripts i and o refer to internal and external properties respectively, and s is the net underpressure in the caisson. The internal and external vertical stresses are deter-

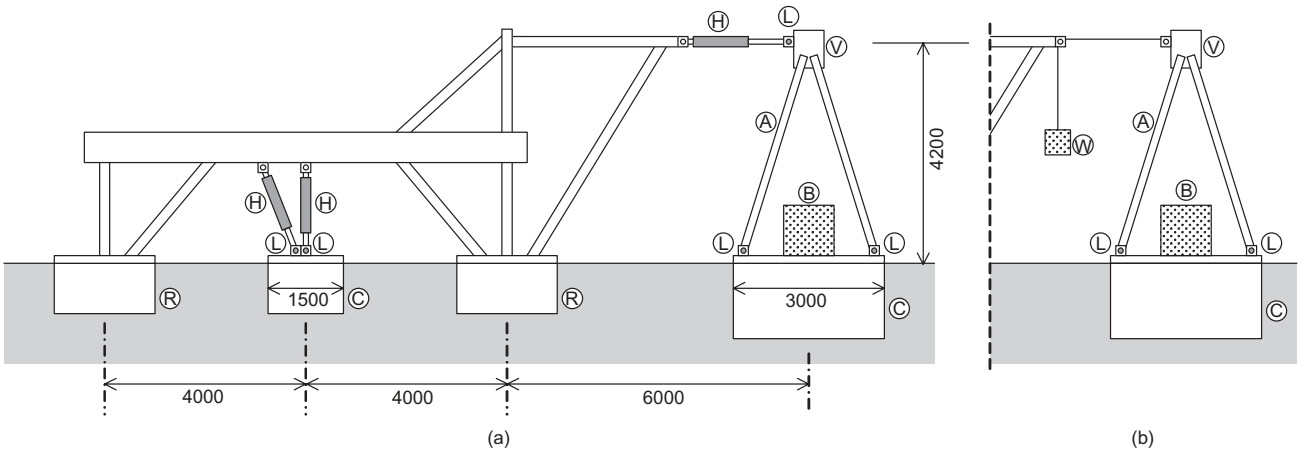

Fig. 4. Outline of field testing equipment, dimensions in mm (water level and displacement reference frames not shown): (a) arrangement for jacking tests on 1·5 m and 3·0 m caissons; (b) alternative arrangement during SEMV tests. A, A-frame; B, concrete block; C, caissons; H, hydraulic jacks; L, load cells; R, foundations of reaction frame; V, SEMV; W, weight providing offset load for SEMV tests

Fig. 5. Test rig showing the 1·5 m caisson installed in foreground and 3·0 m caisson in background after a jacking test had been completed

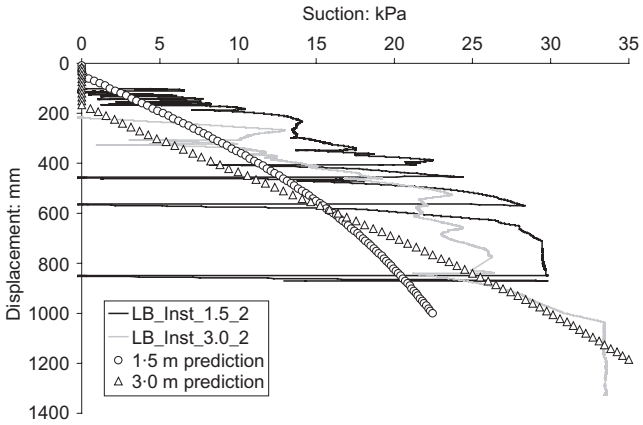

Fig. 6. Records of suction during penetration

mined by numerical integration to account for the modification of the effective unit weight by hydraulic gradients set up in the soil due to the applied suction as well as other assumptions about the stress distribution in the soil. The reader is referred to Houlsby & Byrne (2005) for further details of this formulation. In equation (1) the value of V' must be adjusted for buoyancy, as increasing amounts of the caisson become submerged as the penetration proceeds. The basic parameters used in the calculations presented here were a soil friction angle of 45°, $K\tan\delta = 1$ and an effective unit weight of 10·3 kN/m^3. The vertical load, including self-weight, applied to the caissons was 7 kN and 60 kN for the 1·5 m and 3·0 m diameter caissons respectively. Using these values, the final pressure for installation

Table 1. Outline of caisson tests carried out at Luce Bay

Caisson	Installation	Test type	Code	Notes
1·5 m	1	Installation Jacking test Pull out	LB_Inst_1·5_1 LB_Jack_1·5_1 LB_Pull_1	Combined vertical and horizontal loading: unsuccessful because of control problems
	2	Installation Jacking test Pull out	LB_Inst_1·5_2 LB_Jack_1·5_2 LB_Pull_2	Vertical loading only
3·0 m	1	Installation SEMV tests Jacking test	LB_Inst_3·0_1 LB_SEMV_1 LB_Jack_3·0_1	With offset weight (asymmetric cycling) Increased amplitude cycling
	2	Installation SEMV tests Jacking test	LB_Inst_3·0_2 LB_SEMV_2 LB_Jack_3·0_2	Without offset weight (symmetric cycling) Multiple cycles at each amplitude

of the 3 m diameter caisson is predicted closely, whereas the final pressure required to install the 1·5 m diameter caisson is underpredicted. During the actual installations there were a number of stoppages in pumping for a variety of reasons. It was observed that, after each stoppage, significant downward movements only occurred once the suction returned to a value similar to that before the stoppage.

Figure 7 shows the excess pore pressure measured by sensors placed inside the caissons, 50 mm above the tip of the skirts, plotted against suction measured immediately beneath the lid of the caisson. Although there is some scatter, related largely to the stoppages, there is a strong correlation between the two pressures, as would be expected. In both tests 65% of the suction pressure is measured near the tip of the skirts, and this fraction appears to remain constant throughout the installations. A trend line reflecting this relationship is plotted in the figure.

Figure 8 shows a comparison between the volume of air and water removed from the caisson (by integration of the flow measurement) and the volume computed from the cross-sectional area of the caisson multiplied by the depth of penetration. There is a close relationship between the two. It can be concluded that during the installation (a) little heave occurred within the caisson, and (b) the volume of water seeping through the sand was small. Either of the above phenomena would have resulted in significantly larger volumes from the flow measurements.

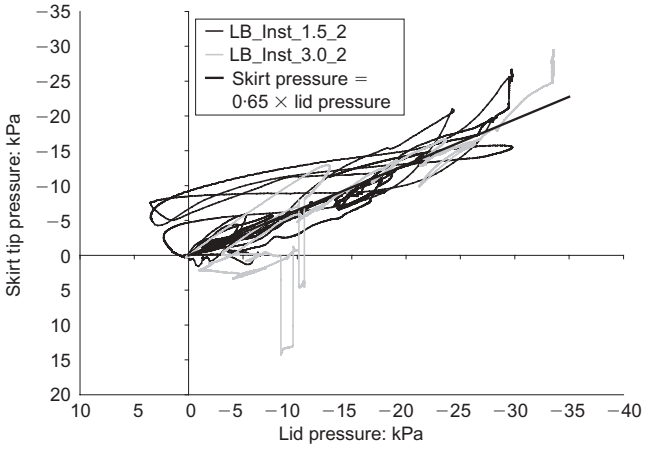

Fig. 7. Relationship between excess pore pressure measured at caisson tip and applied suction to caisson

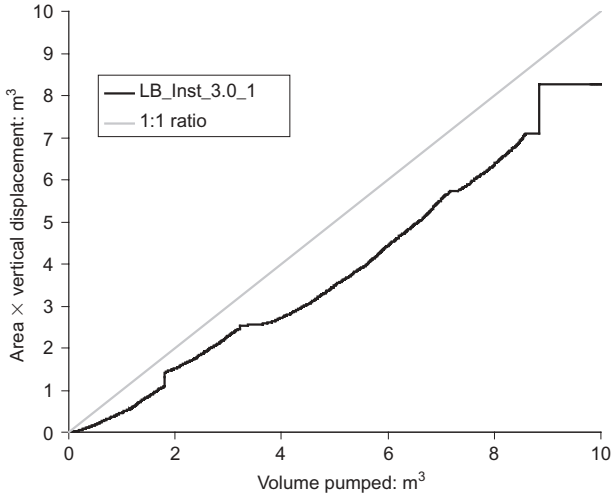

Fig. 8. Relationship between volume pumped from caisson and installed volume

Vibration tests on 3·0 m caisson

Figure 9 shows the record of the applied moment (deduced from the load cells in the legs of the A-frame) against time for an SEMV test in which the excitation is ramped to a constant frequency of 8 Hz and held for about 18 s. As the eccentric masses on the SEMV start to rotate, it exerts an inertial force at the top of the A-frame that varies with the square of the angular velocity. The amplitude of loading therefore builds up parabolically with the frequency. Note that the counter-rotation of the eccentric masses within the SEMV unit produces a symmetric moment time excitation on the foundation.

Figure 10 shows results demonstrating the moment–rotation response, and was compiled by extracting data from a number of tests, each similar to the one shown in Fig. 9, but at different frequencies. From each test the steady-state response has been extracted. The small-amplitude cycles (at frequencies less than 6 Hz) are not shown, as the movements induced in the caisson were too small to be accurately recorded by the accelerometers. As the amplitude of moment increases the moment–rotation loop opens up gradually, until the steady state of 10 Hz cycling is reached, at which stage an approximately elliptical loop is continually retraced. The open loop arises from damping that has three possible causes

(*a*) viscous material damping
(*b*) plastic dissipation of energy in the soil
(*c*) radiation damping.

The minor axes of these ellipses are much smaller than

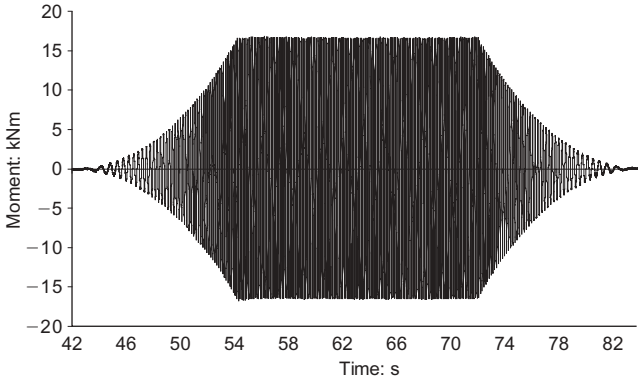

Fig. 9. Moment against time for 8 Hz ramp phase of SEMV test LB_SEMV_2

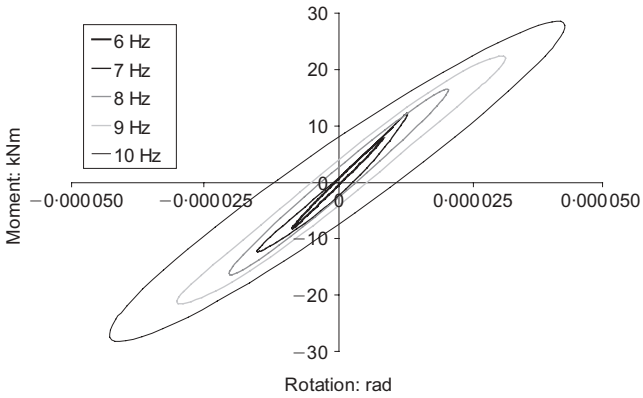

Fig. 10. Moment–rotation response of caisson in test LB_SEMV_2 at progressively higher amplitudes (and frequencies) of loading

those recorded at Bothkennar, indicating that much less damping occurs in dense sand than in soft clay.

The data can be interpreted by first taking the fast Fourier transform (FFT) of both the moment and rotation signals to convert to the frequency domain, and then taking the ratio between the two FFTs to obtain the complex, frequency-dependent 'impedance' (a generalised form of the rotational stiffness). The real part of the impedance represents stiffness and inertial effects, and the imaginary part the damping. At Bothkennar, the main information on the effects of frequency on the response was obtained from the transients at the beginning and end of the test, whereas at Luce Bay the information was gathered from the steady state of individual tests, stepped at 1 Hz intervals from 1 Hz to 10 Hz. Fig. 11 shows the real and imaginary parts of the transfer function computed from 5 Hz to 10 Hz. Also shown as discrete points are the average responses computed at each steady state. The averaged points can be regarded as much more reliable, as they are derived from far more data, but it can be seen that in fact the transfer function deduced from the transient response agrees well with the averaged points.

The data may be compared with theories for the behaviour of a circular foundation on an elastic material. As discussed by Houlsby *et al.* (2005c), Wolf (1994) describes two lumped-parameter models for this case, a three-parameter model and a five-parameter model. Note that these models are derived for the surface footing case, and although not directly applicable to embedded footings, they can be used to assess relative values of deduced moduli. The fitted response from a three-parameter model is shown in Fig. 11 for comparison with the test data, computed for $G = 85$ MPa and $\nu = 0{\cdot}2$. Examining first the real part, the stiffness is chosen to provide a reasonable fit to the data at frequencies in the range 5–6 Hz, but overestimates the stiffness at higher frequencies. This is of course consistent with the common observation that the stiffness of soils reduces with strain amplitude, so that a constant-stiffness model cannot fit behaviour across a wide range of strain amplitudes. At 6 Hz the amplitude of rotation is about 2×10^{-5} rad (see Fig. 10), so the implication is that non-linearity is significant at rotations above this magnitude. No fit from a five-parameter model is shown in Fig. 11, as the five-parameter model gives a very similar variation of the real part of the impedance to the three-parameter model. However, within the range of frequencies tested, the five-parameter model gives a much lower imaginary part of the impedance (representing the damping), therefore the three-parameter model appears to provide a more satisfactory fit to the data. Further discussion about the choice between a three- or five-parameter model and the underlying assumptions of the two models is given in Houlsby *et al.* (2005c).

Jacking tests on 3·0 m caisson

Following the SEMV tests, the 3·0 m caisson was subjected to further cycles of moment, but under quasi-static conditions, by loading with a hydraulic jack (Fig. 4(a)). Fig. 12 shows the moment–rotation curve for cycles from test LB_Jack_3·0_1. The moment–rotation response is initially stiff, with little hysteresis. At larger amplitudes of rotation the secant stiffness decreases and hysteresis increases as the amplitude increases. The cycles at very large amplitude have a characteristic shape in which, after an initially stiff unloading, a very flexible response is observed, followed by slight stiffening. This behaviour is typical of a 'gapping' response in which the stiffening occurs as the gap created during the previous half cycle is closed. Gaps were observed down the side of the caisson during these cycles.

The moment–rotation curve for jacking test LB_Jack_3·0_2 is shown in Fig. 13. In this test packets of 10 cycles were applied to the caisson with amplitudes of ±42 kNm, ±85 kNm, ±169 kNm and ±254 kNm. As for the data in Fig. 12, the displacement amplitude increases with load amplitude, and hysteresis occurs during the larger-amplitude cycles. The unload–reload parts of the curve in Fig. 13 are much stiffer than those shown in Fig. 12. The exact stiffness at these points is difficult to determine accurately owing to an inadequate sampling frequency. As the tests were primarily displacement controlled the load changes very quickly at points of high stiffness. A faster logging rate might have allowed a better definition of the response in the high-stiffness sections. The apparent 'nega-

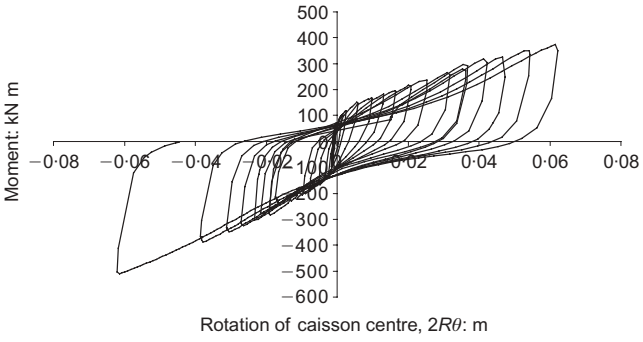

Fig. 12. Moment–rotation curve for loading of 3·0 m caisson, test LB_Jack_3·0_1

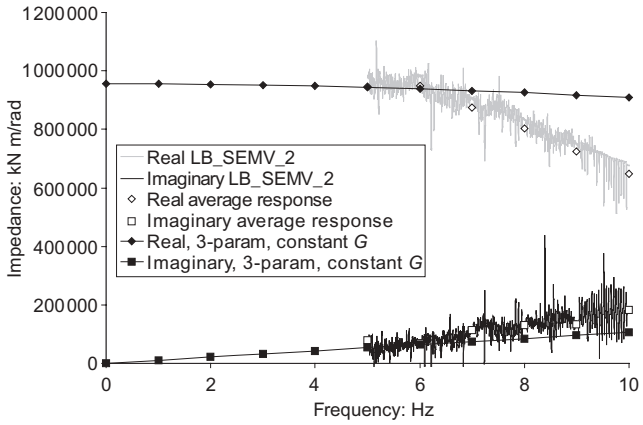

Fig. 11. Complex θ–M transfer function for test LB_SEMV_2

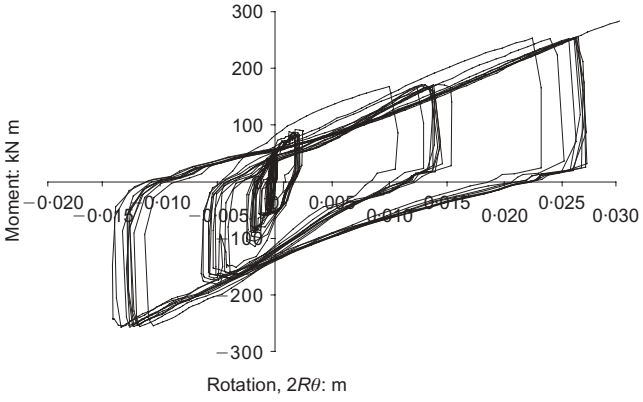

Fig. 13. Moment–rotation curve for loading of 3·0 m caisson, test LB_Jack_3·0_2

tive' stiffness at some stages is almost certainly an artefact of the instrumentation, and is indicative solely of a very stiff response. There is a slight shakedown apparent in the data at low amplitudes of rotation, with a slight stiffening occurring over several cycles of the same amplitude. The moment–rotation response during each packet of cycles appears to approach a steady state by the end of the packet. Byrne & Houlsby (2004) have made similar observations about hysteretic behaviour during cycling from small-scale moment loading tests on caissons in the laboratory.

The SEMV and jacking tests may be compared by deducing the equivalent secant shear modulus from the moment–rotation response of the footing using standard formulae for response of a surface footing to moment loads. Two analyses are required, as discussed in detail by Houlsby *et al.* (2005c): (a) a dynamic analysis for the SEMV tests, and (b) a static analysis for the jacking tests. For the SEMV tests the moment range is taken as the difference between the maximum and minimum values in any given cycle, and the corresponding rotations are computed. The secant stiffness can then be expressed as a function of amplitude of rotation, as shown in Fig. 14. Also shown in Fig. 14 are the secant stiffness values from jacking test LB_Jack_3·0_1. These are consistent with the SEMV data in that they show a continuing reduction of the stiffness with increasing amplitude of cycling: indeed the shape of the $\log(\Delta\theta)$–G curve is very similar to the familiar pattern for variation of stiffness with strain on a $\log(\Delta\gamma)$–G plot. The rotation of the caisson is of course approximately proportional to the shear strain amplitude in the soil. Finally, Fig. 14 shows a simple fit to the variation of the secant shear stiffness based on the hyperbolic moment–rotation relation $M/k_0\theta = (M_{max} - M)/(M_{max} + AM)$, where k_0 is the initial value of the rotational stiffness, M_{max} is the maximum moment, and $k_0/k_{50} = 2 + A$. The curve is constructed for $k_0 = 1125$ MN m/rad (corresponding to $G_0 = 100$ MPa), $M_{max} = 450$ kN m and $A = 4$.

More accurate interpretation of the moment loading tests could be made by accounting for the embedment in the calculation of stiffness factors (e.g. Doherty & Deeks, 2003), but this would simply reduce the absolute values of the estimated soil stiffness, and not significantly change the relative values in the overall interpretation of the pattern of response.

Jacking tests on 1·5 m diameter caissons

Two jacking tests were conducted on the 1·5 m caisson. Test LB_Jack_1·5_1 involved an application of combined vertical and horizontal loads to the caisson via vertical and inclined jacks. A vertical jack applied the mean vertical load, while the inclined jack provided a cyclic loading component. This test was not successful, as it was not possible to control either the mean or cyclic loads accurately, because the soil/caisson/jack system was sufficiently stiff that the jacks were unable to operate independently of each other.

Cyclic vertical loading was applied to the 1·5 m diameter caisson in Test LB_Jack_1·5_2 about a mean load of 60 kN (not including the self-weight of the caisson). Packets of 10 cycles were applied to the caisson with load amplitudes starting at ±10 kN and increasing in steps of ±10 kN to ±100 kN, and these are shown in Fig. 15. The data show that the secant stiffness decreases as the amplitude of the load increases. Furthermore, the displacements increase markedly during load packets where the caisson was cycled into tension. It is of interest to note that the net displacement after each cycle in the ±100 kN load packet was downward, even though large tensile displacements had occurred during each cycle. The implication of this is that, as long as the mean vertical load is compressive, a caisson foundation cycled into tension will ratchet into the sand rather than out of the sand. However, the data also suggest that caissons should not be loaded in tension for serviceability reasons, as the stiffness of the caisson reduces to a level where foundation movements would render a wind turbine inoperable. The data show that the caisson has a significant cyclic tensile capacity (in excess of −40 kN), but extremely large displacements are required to mobilise this capacity. These data support conclusions made from small-scale laboratory tests (Byrne & Houlsby, 2002; Kelly *et al.*, 2003, 2004), and this comparison was an important objective for the large-scale testing programme.

Pullout tests on 1·5 m caisson

At the end of the jacking tests on the 1·5 m caisson, the caisson was pulled out at a rate of 13·7 mm/min by means of the vertical jack. The results for test LB_Pull_2 are shown in Fig. 16. The tensile load decreased rapidly to about −120 kN, at which point a vent plug in the lid of the caisson was opened to prevent damage to the load cell. The tensile load had not reached a maximum by this stage. The proportion of the tensile load generated by suction pressure inside the caisson is also shown in Fig. 16. The difference between the total load carried by the caisson and the suction load represents the friction acting on the skirts of the caisson.

The frictional load generated on the skirts of the caisson as it was pulled out of the sand is shown in Fig. 17, along with an estimate of the friction computed using equation (2) and described in detail by Houlsby *et al.* (2005b).

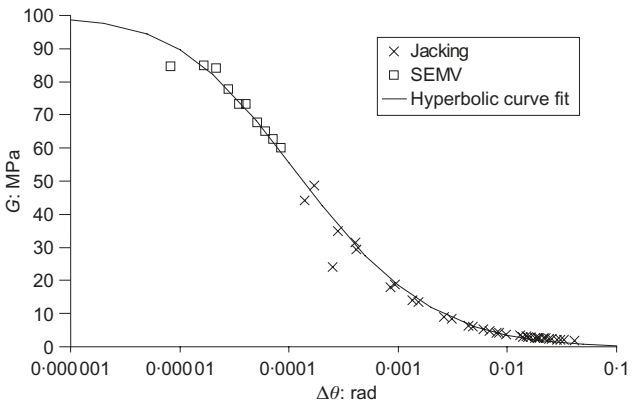

Fig. 14. Computed secant shear modulus from LB_SEMV_2 and LB_Jack_3·0_1

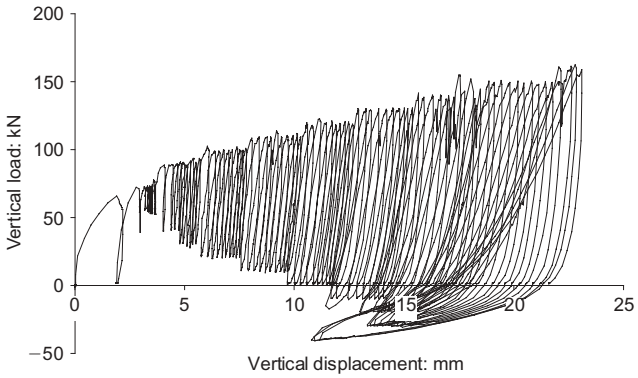

Fig. 15. Cyclic vertical loading of 1·5 m caisson from LB_Jack_1·5_2

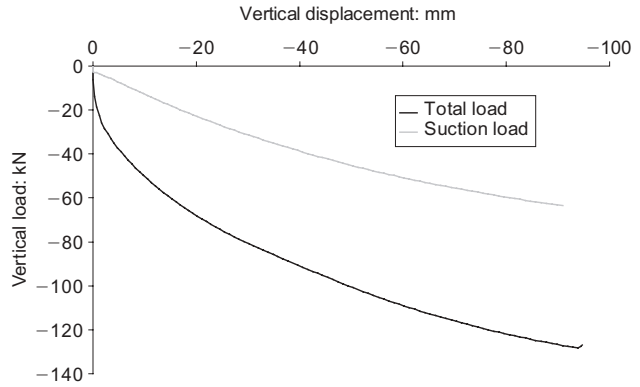

Fig. 16. Load against displacement during pullout test LB_Pull_2

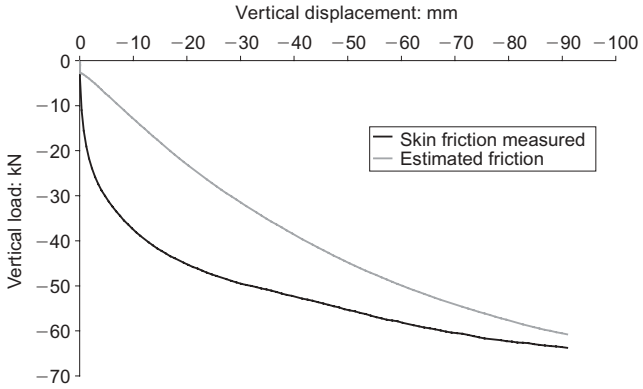

Fig. 17. Measured and computed friction during pullout of 1·5 m caisson in test LB_Pull_2

$$V' = -\left(\frac{s}{h}\right) Z^2 \left(\frac{h}{Z} + \mathrm{e}^{-h/Z} - 1\right) (K \tan\delta)(\pi D) \qquad (2)$$

In this equation s is the net underpressure in the caisson, and $Z = D(m^2 - 1)/(4K \tan\delta)$, where m is the multiple of the diameter over which the vertical stress is reduced owing to the friction on the outside of the caisson skirt (i.e. $D_m = mD$); a value $m = 2{\cdot}0$ has been used in the calculations. This calculation is based on principles similar to that used to predict the suction during installation shown in Fig. 6, and the parameters used in the two calculations are similar. The fit to the measured data is poor for small displacements but converges towards the end of the pullout.

IMPLICATIONS FOR FULL-SCALE FOUNDATIONS

The principal purpose of the tests described here is for calibration of 'force resultant' theoretical models based on work-hardening plasticity to describe the response of caisson foundations (Houlsby, 2003). However, some simple scaling can be applied to the results of the tests to make some preliminary estimates of the sizes of caissons that would be needed for full-scale wind turbine installations.

A 3·5 MN wind turbine in typical offshore conditions would result in an overturning moment, in extreme conditions, of approximately 120 MN m (Byrne & Houlsby, 2003). If at this stage it is determined that (say) an acceptable two-way rotation of the foundation is 0·002 rad, then the results from Fig. 14 indicate that for this rotation the shear modulus would be about 15 MPa. We assume that, at similar rotations, the shear strains in the soil will be similar, so that at a particular rotation we can scale modulus with pressure, but do not need to adjust the modulus for its well-known dependence on strain amplitude. If it is assumed that the shear modulus scales with the square root of the mean stress, then it can be estimated that a caisson of diameter 20 m would be required to provide a sufficiently stiff response in sand with a relative density of about 80%. The cyclic nature of the applied loading is due principally to the waves, which may have a period of about 10 s. For this case the dimensionless frequency $a = \omega R/c_s$ (where ω is the frequency, R is the caisson radius and c_s is the shear wave velocity = 200 m/s) would be about 0·03, indicating that the dynamic effects would be minimal (Wolf, 1994), and a quasi-static analysis of the foundation would be fully justified.

If alternatively an approach based on strength were adopted, then it may be estimated that the 3·0 m caisson would be able to sustain cyclic moments of about 0·12 MN m without significant degradation of response. As the moment capacity scales linearly with the effective unit weight, and with the fourth power of the foundation size, it is concluded that a foundation of 17 m diameter would be required in sand with an effective unit weight of 10·3 kN/m^3 with similar properties to that at Luce Bay. Byrne & Houlsby (2003) proposed equation (3) as another method for estimating the diameter of a monopod foundation at low vertical loads

$$\frac{M}{2R} = \left(f_1 + \frac{2RH}{M} f_2\right)^{-1} (V + f_3 W) \qquad (3)$$

where M is the overturning moment, R is the radius of the caisson, H is the horizontal load, V is the vertical load, and W is the effective weight of the sand inside the caisson. The factors f_1, f_2 and f_3 were obtained from a limited number of small-scale laboratory tests, and are equal to 3·26, 1·07 and 0·71 respectively. If the weight of the structure was 6 MN and the horizontal load was 4 MN then equation (3) indicates that the diameter of the monopod foundation would be about 19 m if the ratio of the length of its skirt to its diameter were 0·5.

Either the strength or the stiffness criterion therefore results in a foundation of comparable size, but the latter, which is related to serviceability considerations (i.e. deformations), leads to a requirement for a slightly larger foundation.

If a quadruped were to be designed then, first, the caisson spacing must be determined. For an overturning moment of 120 MN m and a weight of the structure of 6 MN, then a spacing of 40 m is needed if tension is to be avoided completely. The confirmation on the basis of large-scale tests that tension should be avoided is considered an important, though negative, outcome from this research. The maximum loading on an individual caisson would be 3 MN, which could be carried in sand like that at Luce Bay with a factor of safety of about 1·5 by a caisson of diameter 3·5 m. The estimated shear load of 4 MN can be carried by a caisson with a diameter of 4 m and a skirt length of 2·67 m. In this case the shear loading appears to govern the size of the caisson required, but it is considered likely that this would change when deformations are taken into account. Unfortunately, however, it is difficult to assess the influence the caisson size would have on the overall stiffness of the structure, without more detailed knowledge of the structure itself.

A comparison of the estimated caisson diameters for a wind turbine foundation in dense sand with those estimated for soft clay by Houlsby *et al.* (2005c) shows that the size of a mono-caisson foundation in dense sand would be about

60% of that in soft clay, whereas the sizes of caissons in a quadruped foundation would be rather similar.

CONCLUSIONS

A series of field trials of caisson foundations in sand is described. The tests are relevant to the design of both monopod and quadruped foundations for offshore wind turbines. Installation of the caissons was achieved by suction. High-frequency, low-amplitude cyclic moment tests on a 3·0 m caisson showed that the response was affected by stiffness, inertial and damping effects. Low-frequency cyclic moment tests on the 3·0 m caisson indicated a stiff response at low amplitude, with a gradual reduction of stiffness and increase of hysteresis at large amplitude. There was evidence of gapping at the side of the caisson under very large-amplitude cycles. Cyclic vertical loading tests on a 1·5 m diameter caisson also showed a reduction of stiffness and increase of hysteresis as load amplitude increased, with a significant reduction in stiffness after the compression to tension boundary was crossed and frictional capacity exceeded. Pullout of the 1·5 m caisson indicated that a sizeable ultimate tensile resistance can be generated but is accompanied by extremely large displacements. The tests contribute to the development of design procedures for offshore wind turbines founded on caissons.

ACKNOWLEDGEMENTS

This research was sponsored by the Department of Trade and Industry and a consortium of companies (Fugro Ltd, SLP Engineering Ltd, Garrad Hassan, General Electric Wind Ltd, Aerolaminates Ltd and Shell Renewables Ltd). The authors are very grateful to Mr Adam Macintosh of Luce Bay Plant Hire for making the site available for this testing. The authors thank Dr A. Blakeborough for use of the SEMV designed by him, and for advice on interpretation of the SEMV tests. Dr B.W. Byrne acknowledges the support provided by Magdalen College, Oxford.

NOTATION

A parameter in equation for stiffness variation
a dimensionless angular velocity
c_s shear wave velocity in sand
D diameter of caisson
f_1, f_2, f_3 empirical factors in moment capacity equation
G shear modulus of soil
H horizontal load on caisson
h skirt length of caisson
k rotational stiffness
$K \tan \delta$ factor relating shear stress on caisson wall and vertical stress
K_0 coefficient of earth pressure at rest
M overturning moment on foundation
M_{max} limiting overturning moment
m stress distribution factor for installation/extraction analysis
N_q bearing capacity factor (overburden)
N_γ bearing capacity factor (self-weight)
p_a atmospheric pressure
p' mean effective stress
R radius of caisson
s net underpressure in caisson
t caisson skirt wall thickness
V vertical load on caisson
V' effective vertical load on caisson
W effective weight of soil plug within caisson
z depth from soil surface
γ shear strain
γ' effective unit weight of soil
θ rotation of foundation due to overturning moment
ν Poisson's ratio
σ'_v vertical effective stress
ω angular velocity of dynamic excitation

REFERENCES

Byrne, B. W. & Houlsby, G. T. (2002). Experimental investigations of the response of suction caissons to transient vertical loading. *Proc. ASCE, J. Geotech. Engng* **128**, No. 11, 926–939.

Byrne, B. W. & Houlsby, G. T. (2003). Foundations for offshore wind turbines. *Phil. Trans. R. Soc. of London Ser. A*, **361**, Dec., 2909–2930.

Byrne, B. W. & Houlsby, G. T. (2004). Experimental investigations of the response of suction caissons to transient combined loading. *Proc. ASCE, J. Geotech. Geoenviron. Engng* **130**, No. 3, 240–253.

Doherty, J. P. & Deeks, A. J. (2003). Elastic response of circular footings embedded in a non-homogeneous half-space. *Géotechnique* **53**, No. 8, 703–714.

Houlsby, G. T. (2003). Modelling of shallow foundations for offshore structures: invited theme lecture. *Proceedings of the international conference on foundations*, Dundee, pp. 11–26.

Houlsby, G. T. & Byrne, B. W. (2005). Design procedures for installation of suction caissons in sand. *Proc. ICE Geotech. Engng* **158**, No. 3, 135–144.

Houlsby, G. T., Ibsen, L.-B. & Byrne, B. W. (2005a). Suction caissons for wind turbines. *Proceedings of the international symposium on frontiers in offshore geotechnics*, 75–94. London: Taylor and Francis.

Houlsby, G. T., Kelly, R. B. & Byrne, B. W. (2005b). The tensile capacity of suction caissons in sand under rapid loading. *Proceedings of the international symposium on frontiers in offshore geotechnics*, 405–410. London: Taylor and Francis.

Houlsby, G. T., Kelly, R. B., Huxtable, J. & Byrne, B. W. (2005c). Field trials of suction caissons in clay for offshore wind turbine foundations. *Géotechnique* **55**, No. 4, 287–296.

Houlsby, G. T., Kelly, R. B., Huxtable, J. & Byrne, B. W. (2005d). *Field testing of suction caissons at Bothkennar and Luce Bay*, Report No. OUEL 2276/05. Department of Engineering Science, University of Oxford.

Kelly, R. B., Byrne, B. W., Houlsby, G. T. & Martin, C. M. (2003). Pressure chamber testing of model caisson foundations in sand. *Proceedings of the international conference on foundations*, Dundee, pp. 421–431.

Kelly, R. B., Byrne, B. W., Houlsby, G. T. & Martin, C. M. (2004). Tensile loading of model caisson foundations for structures on sand. *Proceedings of the international symposium on offshore and polar engineering*, Toulon, Vol. 2, pp. 638–641.

Wolf, J. P. (1994) *Foundation vibration analysis using simple physical models*. Englewood Cliffs, NJ: Prentice Hall.